La mer 61 : 19–29, 2023, https://doi.org/10.32211/lamer.61.1-2_19
Société franco-japonaise d'Océanographie, Tokyo

Characteristics of the two types of Kuroshio large meanders

Hiroyuki YORITAKA[1)]*, Atsushi KUBOKAWA[2)] and Kimio HANAWA[3)]

Abstract: There are two types of Kuroshio large meanders: the large meander west (LMW), whose trough (the southernmost point) is located west of the Izu-Ogasawara Ridge, and the large meander east (LME), whose trough is located on the ridge. We compared the characteristics of LMW and LME using accumulated Kuroshio path data. Comparing the five LMWs and three LMEs, the central latitude of the meanders of the LME was higher than that of the LMW, and the amplitude of the meanders of the LME was smaller than that of the LMW. Fitting the solution of the path equation to the Kuroshio path, the initial path direction of the LME was smaller than that of the LMW, but the characteristic velocities and meander wavelengths of the LME were not significantly different from those of the LMW. The difference in longitude between the LME and LMW troughs is due to the difference in separation longitude, not the difference in meander wavelength associated with the difference in characteristic velocity.

Keywords : *Kuroshio, large meander, Rossby lee wave, path equation*

1. Introduction

The Kuroshio in the Shikoku Basin exhibits two modes, namely, a straight path (blue line in Fig. 1) and a large meander path (red line in Fig. 1), as described in STOMMEL and YOSHIDA (1972). Both paths enter the Pacific Ocean from approximately 130° E and 30° N, Tokara Strait south of Kyushu, and pass north of Hachijojima (33° N) on the Izu-Ogasawara Ridge, which extends north-south at approximately 140° E. From the dynamic perspective, ROBINSON and TAFT (1972), using the path equation (ROBINSON and NILLER, 1967), regarded the large meander path as a Rossby lee wave that separated from the continental slope off the south coast of Shikoku (132° E-135° E). WHITE and MCCREARY (1976) regarded the large meander path as a Rossby lee wave generated by bypassing Kyushu. They considered that, since the wavelength of a linear Rossby wave is proportional to the square root of the current velocity, a large meander path exists if the current velocity of the Kuroshio is in the range where the entire large meander path (one and half wavelengths) is shorter than the distance between Kyushu and the Izu-Ogasawara Ridge; the large meander path does not appear if the current velocity is higher than that range.

MASUDA (1982), using the path equation, showed that, within a specific current velocity range, multiple equilibria can exist for which

1) Kuroshio Science Unit, Kochi University, Monobe-Otsu 200, Nankoku, Kochi, 783–8502, Japan
2) Faculty of Environmental Earth Science, Hokkaido University, N10W5, Sapporo, Hokkaido, 060–0810, Japan
3) Yamagata University, Kojirakawa 1–4–12, Yamagata, Yamagata, 990–8560, Japan

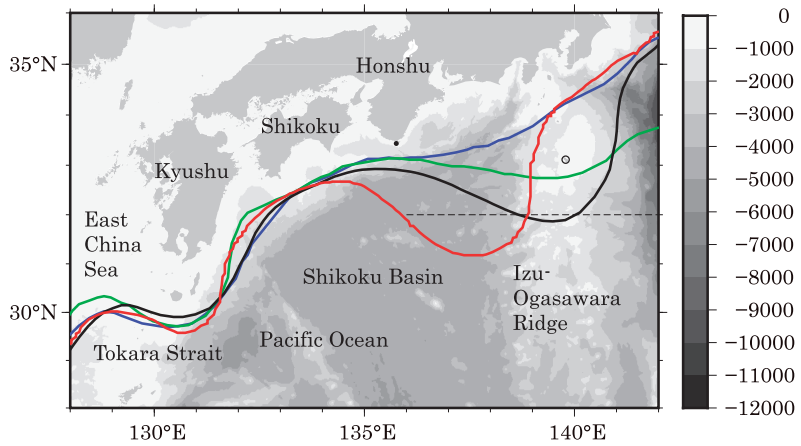

Fig. 1 Map around the Shikoku Basin and the typical path (solid line) for four modes of the Kuroshio path based on the QBOC (Quick Bulletin of Ocean Conditions); the non-large meander north (NLMN: blue), non-large meander south (NLMS: green), large meander east (LME: black), and large meander west (LMW: red). Dashed line indicates 32° N line. Open circle indicates Hachijojima, closed circle indicates Cape Shionomisaki. Color scale is for water depth. ETOPO1 was used for bathymetric data.

there are both straight and large meander paths through the inlet, that is Tokara Strait and outlet of the Izu-Ogasawara Ridge at different latitudes. Subsequently, several regional models driven by inflow and outflow with different latitudes obtained multiple equilibrium solutions in specific velocity ranges (Chao, 1984; Yasuda *et al.*, 1985; Yoon and Yasuda, 1987; Akitomo *et al.*, 1991).

Tsujino *et al.* (2006) and Tsujino *et al.* (2013) drove the ocean general circulation model with historical winds and reproduced the Kuroshio large meander, although it did not necessarily match the actual period of occurrence. Tsujino *et al.* (2013) noted that the meander tended to decay as the Kuroshio transport increased. Usui *et al.* (2013) also showed that Sverdrup transport in the Shikoku Basin increased at the last stage of the historical Kuroshio large meander.

Yoshida *et al.* (2014) statistically analyzed the Kuroshio path in the Quick Bulletin of Ocean Conditions (QBOC) issued by the Japan Coast Guard, and proposed another large meander path (large meander east: LME) whose trough (southernmost point) is located south of 32° N, similar to the conventional large meander path (large meander west: LMW), but with a much different longitude. While the trough of the LMW is located west of the Izu-Ogasawara Ridge, the trough of the LME is located on the ridge. Figure 1 shows typical paths for the four modes of the Kuroshio path classified by Yoshida *et al.* in the QBOC. If the southernmost latitude of 136° E-142° E is north of 32° N, the path is a non-large meander; else, if the southernmost latitude of 136° E-142° E is south of 32° N, the path is a large meander. The non-large meander path passing north of Hachijojima (see Fig. 1) is the non-large meander north (NLMN); the non-large meander path passing south of Hachijojima is the non-large meander south (NLMS); the large meander path passing north of Hachijojima

is the LMW, and the large meander path passing south of Hachijojima is the LME. YOSHIDA *et al.* classified the Kuroshio paths from 1970 to 2009 and showed that the LMW accounted for 23 % in terms of time and the LME accounted for 9 %.

The purpose of this study is to elucidate the differences in the characteristics of the LMW and LME. In particular, we will estimate the characteristic velocities of the LMW and LME by the path equation and investigate whether the velocity of the Kuroshio controls the appearance and disappearance of the LMW, as suggested by WHITE and MCCREARY.

2. Data and method

2.1 Kuroshio path

As the Kuroshio path, the current axis of the Kuroshio path drawn in the QBOC (Quick Bulletin of Ocean Conditions) was used. In the QBOC, the Kuroshio path fixed at a width of 40 nautical miles (approximately 74 km) is drawn based on the analysis of the observed data of current, sea surface temperature, and 200-m-depth temperature. The QBOC has been issued twice a month since April 1960, once a week since April 2001, and daily on weekdays since August 2006. We used the line data created by the Japan Hydrographic Association from the QBOC image data (JAPAN HYDROGRAPHIC ASSOCIATION, 2022). The current axis was defined as the location of 13 nautical miles (approximately 24 km) from the coastal side of the Kuroshio path. In addition, since August 2006, we used only the data issued on Wednesdays, as in the case of the earlier data.

For all modes in Fig. 1, the Kuroshio seems to flow along the coast after entering the Pacific Ocean at 130° E-131° E. For the NLMN, the Kuroshio flows along the coast to near Cape Shionomisaki (135.76° E). For the NLMS, the path has a crest (northernmost point) near Cape Shionomisaki and flows southward at a small angle to the latitude line, and it turns northward with a trough at 139° E-140° E. For the LME, the path leaves the coast at 135° E-136° E as a crest and flows southward, and it turns northward with a trough at 139° E-140° E. For the LMW, the path leaves the coast and flows southward with a crest at 134° E-135° E, and it turns northward with a trough at 137° E-138° E. For both large meander paths, the LME and LMW, the path between the crest and trough has the form of a sine wave, and it is presumed to be a free Rossby lee wave.

Figure 2 shows the mode of the Kuroshio path in the QBOC from 1972 to 2019. There were eight large meander periods of LME or LMW that lasted more than one year (thick solid line in Fig. 2). The 8th large meander period, which began in 2017, continues through 2020 and beyond. Figure 3 shows the Kuroshio paths for each large meander period, and Table 1 shows the appearance frequency of each path mode during each large meander period. LME is dominant in 1999–2001 and 2008–2009; LME and LMW are comparable in 1981–1984 and 1989–1991.

2.2 Path equation and its property

The path equation derived by ROBINSON and NIILER (1967) was used. Assuming that the current velocity at the sea bottom is zero, the path equation can be written as follows:

$$U\left(\frac{d\theta}{dy}-\kappa_0\right)+\beta(Y-Y_0)=0 \qquad (1)$$

where U is the characteristic velocity $\left(\frac{\langle v^2\rangle}{\langle v\rangle}\right)$ (v is the current velocity in the path direction), and $\langle\ \rangle$ denotes the surface integral over the cross-section of the path. θ is the path direction from east, y is the coordinate of the path direction, $\left|\frac{d\theta}{dy}\right|$ is the curvature of the path,

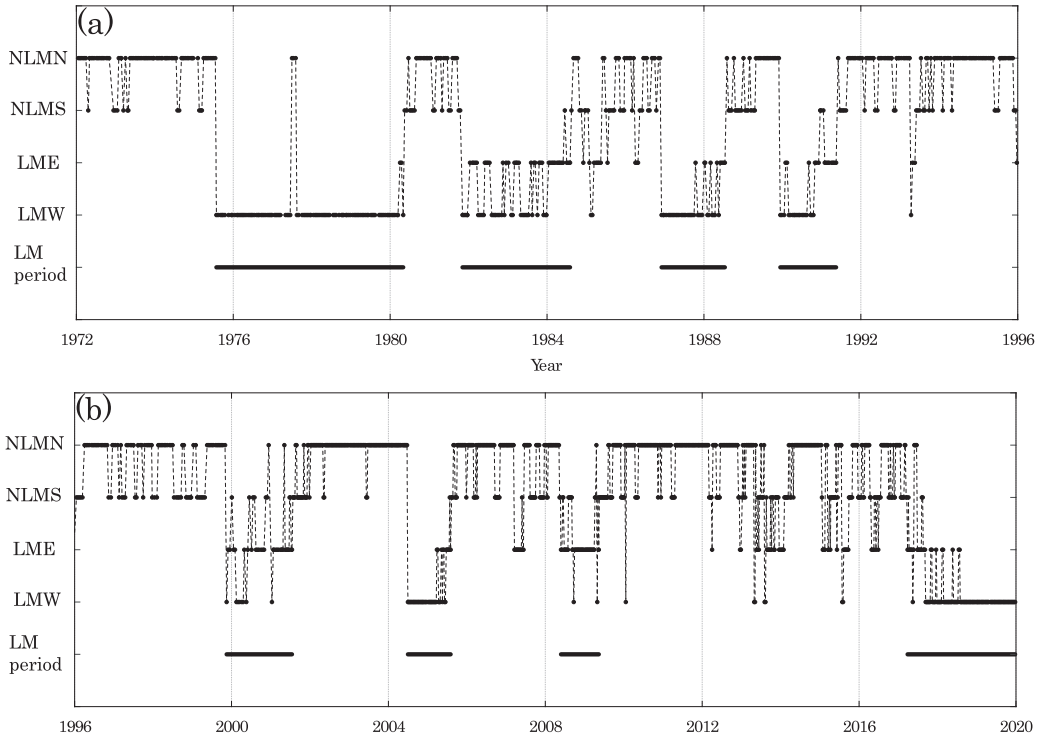

Fig. 2 Mode of the Kuroshio path (small closed circle and dashed line). (a) 1972–1995, (b) 1996–2019. Thick solid line indicates large meander periods of more than one year.

and κ_0 is $\left(\frac{d\theta}{dy}\right)$ at the initial position of the path (X_0, Y_0) (the parameters are shown in Fig. 4). β is the meridional variation $\left(\frac{df}{dY}\right)$ of the Coriolis parameter f. Equation (1) represents the conservation of the potential vorticity of a thin jet, with the first term on the left side representing the relative vorticity, and the second term on the left side representing the planetary vorticity. The characteristic velocity coincides with the current velocity if the current is spatially uniform, and when the velocity has a jet-like profile, it is positively correlated with the maximum velocity, but it is much lower than the maximum velocity. Robinson and Taft (1972) varied the characteristic velocity of the Kuroshio in the Shikoku Basin in the range of 0.2–1.0 m/s and tried to change the path. Assuming that the initial curvature is zero, the path is determined by the initial path direction θ_0 and the characteristic velocity U. Figure 5 shows the variation in the path due to the variation in the initial path direction θ_0 and the characteristic velocity U. If the initial path direction is in this range, the form of the path is close to a sine wave, and the larger the initial path direction, the larger the amplitude and the shorter the wavelength. On the other hand, the higher the characteristic velocity, the larger the amplitude and the longer the wavelength is.

A steady jet with a north-south component follows the path equation if there is no generation or dissipation of vorticity owing to contact with the lateral or bottom boundary. Then, the jet

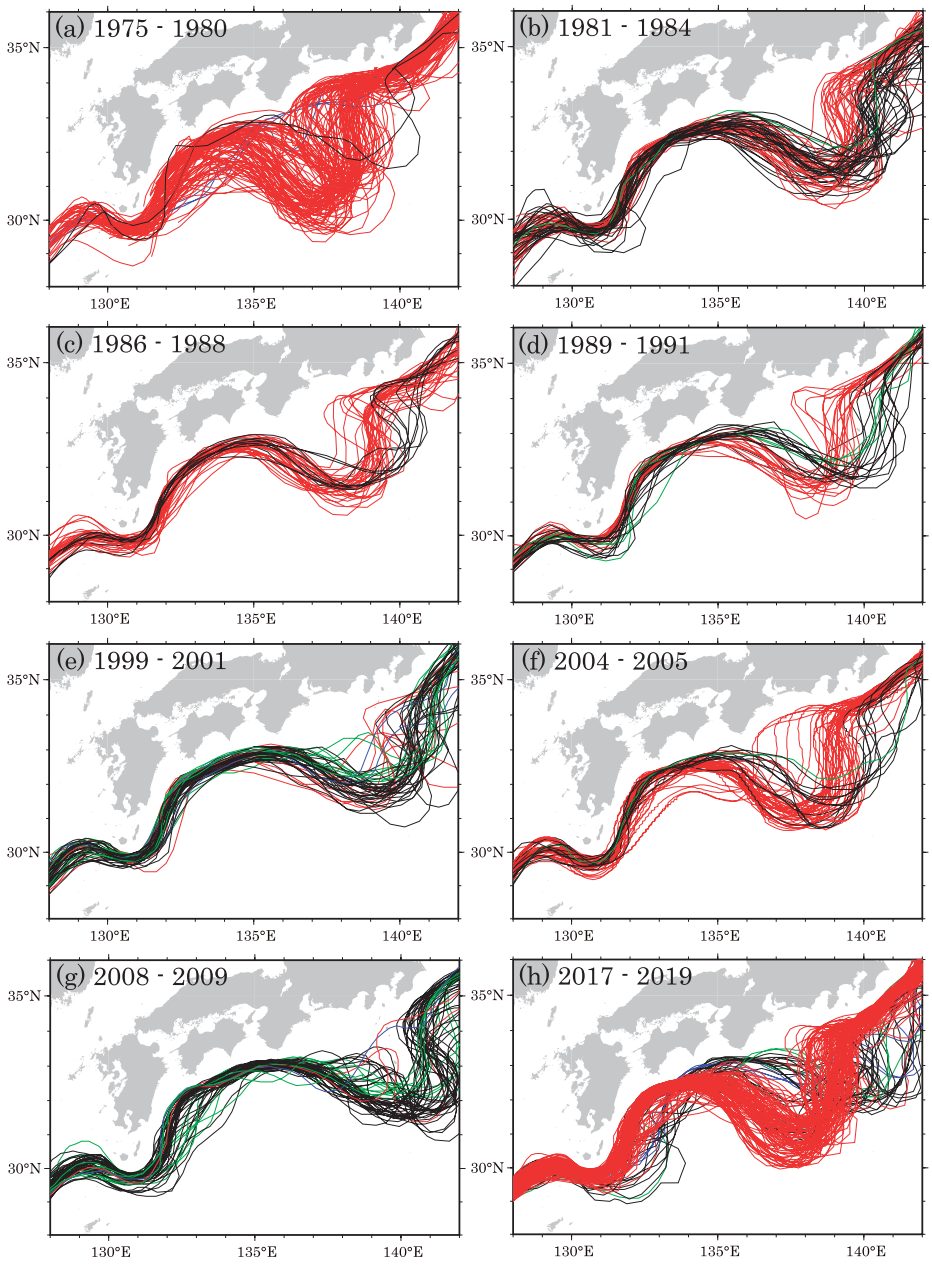

Fig. 3 Kuroshio path based on the QBOC. NLMN (blue), NLMS (green), LME (black), and LMW (red).

heads east while meandering as a Rossby lee wave. This equation does not allow us to discuss the path near the lateral boundary or in shallow waters, and therefore, we cannot definitely state how the western boundary current separates from the lateral boundary. However, considering that the western boundary current flowing from the south along the boundary separates

Table. 1 Appearance frequency of each path mode during each large meander period.

No	Period	Frequency of each path mode			
		NLMN	NLMS	LME	LMW
1	1975 Jul. - 1980 May	3	0	2	102
2	1981 Nov. - 1984 Aug.	0	1	35	30
3	1986 Dec. - 1988 Jul.	0	0	9	31
4	1989 Dec. - 1991 May	0	3	14	18
5	1999 Nov. - 2001 Jul.	2	8	30	8
6	2004 Jun. - 2005 Aug.	0	1	11	44
7	2008 May - 2009 May	1	10	37	2
8	2017 Mar. - 2019 Dec.	4	3	24	112

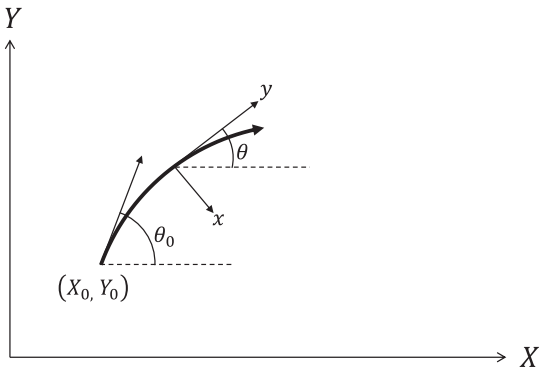

Fig. 4 Parameters in the path equation.

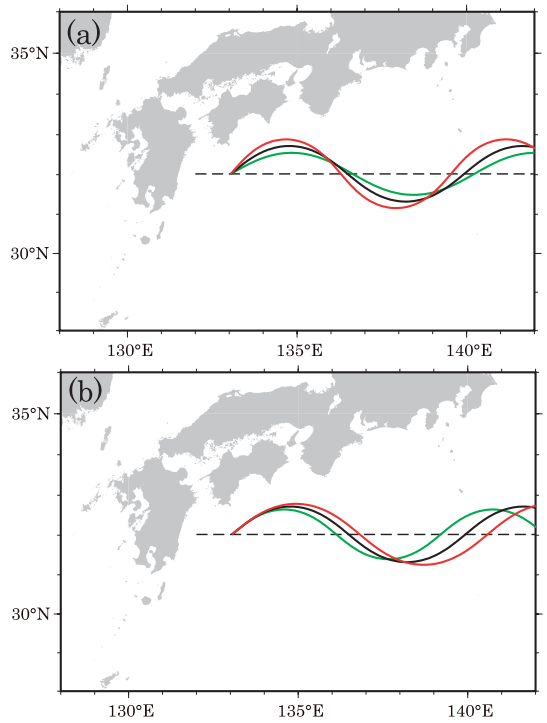

Fig. 5 Variation in the solution of the path equation due to changes in (a) the initial path direction 30° (green), 40° (black) and 50° (red) for the characteristic velocity 0.25 m/s, and (b) the characteristic velocity 0.20 m/s (green), 0.25 m/s (black) and 0.30 m/s (red) for the initial path direction 40°.

from the boundary as the relative vorticity decreases due to the β effect, as shown in Fig. 6, the latitude of separation point is Y_0 where the path has zero curvature, and the boundary direction becomes the initial path direction θ_0. The separation point is the point where vorticity is supplied by contact with the boundary immediately upstream and potential vorticity is conserved downstream of it.

3. Characteristics of large meanders

Figure 7 shows the ten mean paths for the eight large meander periods shown in Table 1, along with their standard deviations at the crests and troughs; for 1981–1984 and 1989–1991, the mean paths of both the LMW and LME were determined. The mean path was determined as the mean latitude of the path for every 0.05 degrees of longitude from 128° E to just east of the trough. The mean was taken by excluding the paths farthest from the mean path until all paths were within 0.8 degrees of latitude from the mean path. The horizontal broken lines in Fig. 7 are the central latitudes of the crest and trough of each mean path. In our model shown in Fig. 6, the central latitude coincides with the latitude of the separation point, because the curvature of the path is zero there. The 2000 m isobath east of Kyushu and south of Shikoku extends approximately 60 degrees (from the east) south of 31.5° N and approximately 30 degrees (from the east)

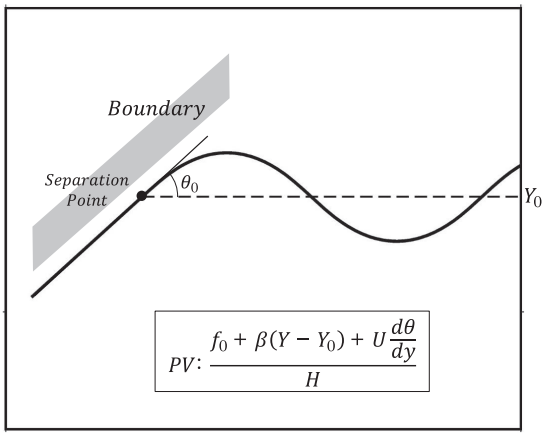

Fig. 6 Schematic diagram of the separation of the western boundary current and the Rossby lee wave. PV denotes the potential vorticity of the thin jet separated from the coast, f_0 denotes the Coriolis parameter at Y_0, β denotes the meridional variation of the Coriolis parameter, U denotes the characteristic velocity, and H denotes the height of the water column, which is constant along geostrophic streamlines in the one-layer reduced gravity model. $Ud\theta/dy$ is the relative vorticity. The parameters are shown in Fig. 4.

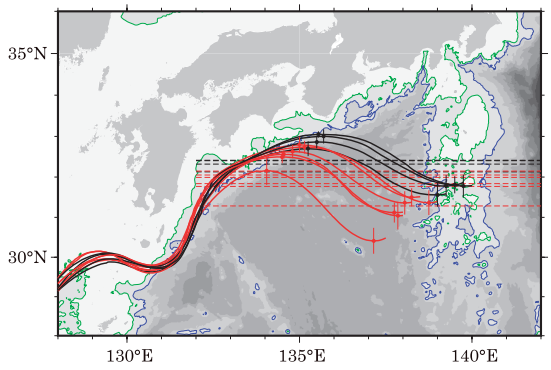

Fig. 7 Mean path (solid line) and central latitude (dashed line) of the Kuroshio path. The circles indicate the crests and troughs, and the thin vertical lines indicate standard deviations at the crests and troughs. LME (black), and LMW (red). The green line indicates the 1000 m isobath and the blue line indicates the 2000 m isobath. Color scale of water depth is same as in Fig. 1.

north of 31.5° N. The mean path of the large meander, except for 1975–1980 (LMW), seems to lie on the 2000 m isobath south of 31.5° N, and on the 1000 m isobath south of Shikoku. The separation point is the intersection of the central latitude and the mean path. The five LMW separation points, except 1975–1980, are on the transition from the 2000 m isobath to the 1000 m isobath, and the three LME separation points, except 1981–1984, are on the 1000 m isobath south of Shikoku.

Figure 8 shows the optimal solution of the path equation fitted to the path between the crest and trough for each mean path (Fig. 7). The solution of the path equation has zero curvature at the central latitudes of the crest and trough of the mean path. By varying the initial path direction θ_0 in steps of 1 degree, the characteristic velocity U in steps of 0.01 m/s, the combination of initial path direction and characteristic velocity that minimizes the root-mean-square difference in latitude between the mean path and the solution between the crest and trough in the mean path was determined. Figure 8 shows that the solution of the path equation does not fit the mean path in the west of the crest except 1975–1980 period. The paths seem to lie on the 1000 m isobath south of Shikoku, which elongates the length between the separation point and the crest. Although the details are unclear, it seems that the continental slope strongly affects the path through a mechanism not considered in the thin jet theory.

Table 2 shows the parameters of the optimal solution. As typical values of LMW, we use the mean of the five LMW except for 1975–1980, and as typical values of LME, we use the mean of the three LME except for 1981–1984. Table 2 shows the mean and standard deviation for LMW and

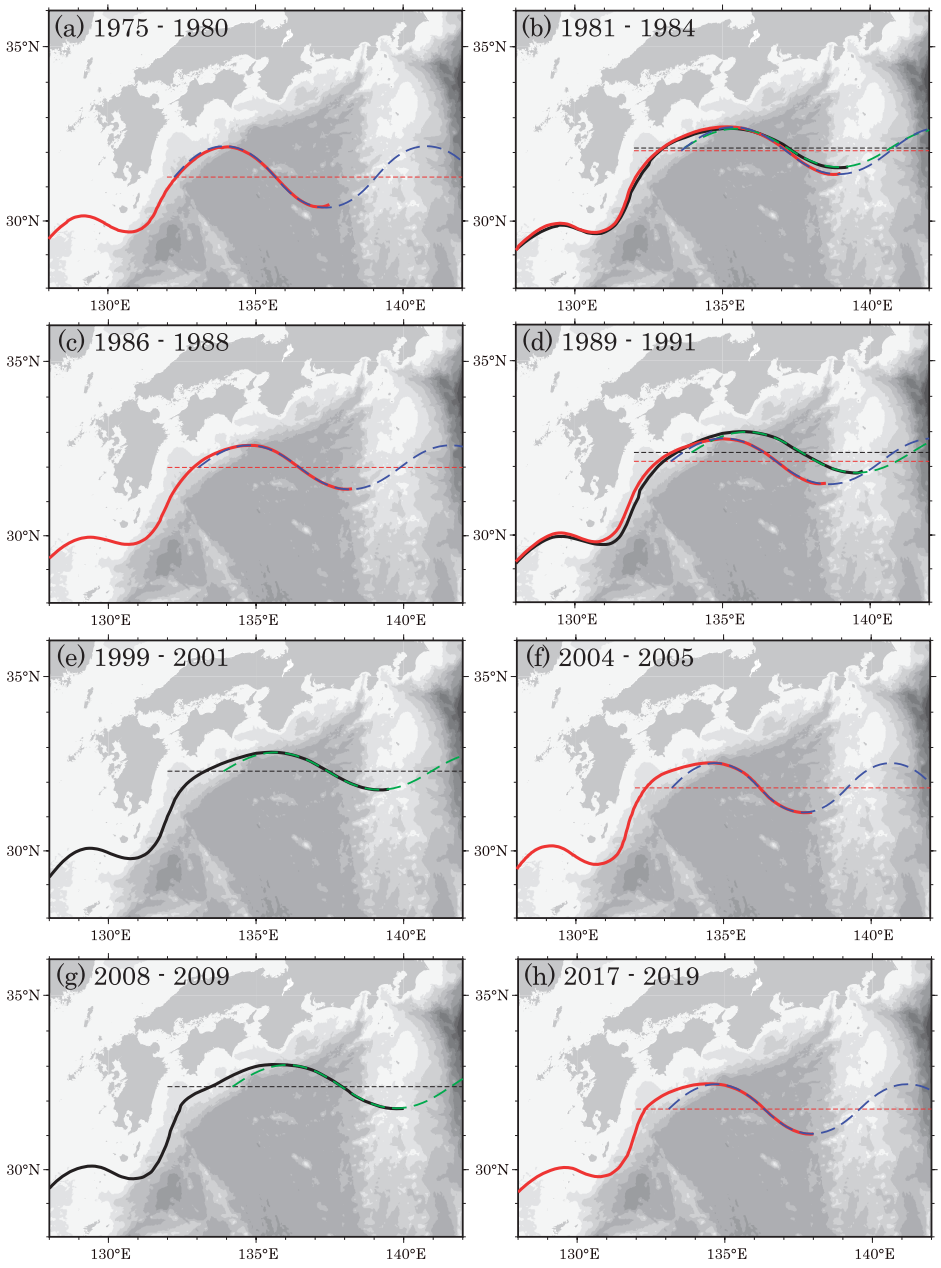

Fig. 8 Optimal solution (dashed line) of the path equation fitted to the mean path of the Kuroshio (solid line). Thin dashed line indicates the central latitude. Black and green lines indicate LME; red and blue lines indicate LMW. Color scale of water depth is same as in Fig. 1.

Table. 2 Parameters of optimal solution.

Period	Mode	Central latitude [degrees]	Amplitude [degrees]	Initial path direction [degrees]	Characteristic velocity [m/s]	Trough longitude [degrees]	Seperation longitude [degrees]	3/4Wave-length [degrees]	Elongation [degrees]
1975 - 1980	LMW	31.29	0.89	49	0.28	137.37	132.32	5.12	-0.07
1981 - 1984	LMW	32.05	0.68	38	0.26	138.92	132.84	5.32	0.76
1986 - 1988	LMW	31.99	0.64	37	0.24	138.18	132.88	5.13	0.17
1989 - 1991	LMW	32.15	0.66	37	0.26	138.60	132.82	5.35	0.43
2004 - 2005	LMW	31.84	0.71	46	0.20	137.70	132.37	4.45	0.88
2017 - 2019	LMW	31.77	0.72	43	0.23	137.95	132.30	4.85	0.80
Mean for LMW		**31.96**	**0.68**	**40**	**0.24**	**138.27**	**132.64**	**5.02**	**0.61**
Standard deviation		**0.15**	**0.03**	**4**	**0.02**	**0.49**	**0.28**	**0.38**	**0.30**
1981 - 1984	LME	32.13	0.55	32	0.24	138.94	133.00	5.24	0.70
1989 - 1991	LME	32.40	0.59	32	0.27	139.54	133.45	5.59	0.50
1999 - 2001	LME	32.32	0.54	31	0.24	139.18	133.28	5.28	0.62
2008 - 2009	LME	32.41	0.62	34	0.27	139.74	133.47	5.54	0.73
Mean for LME		**32.38**	**0.58**	**32**	**0.26**	**139.49**	**133.40**	**5.47**	**0.62**
Standard deviation		**0.05**	**0.04**	**2**	**0.02**	**0.28**	**0.10**	**0.17**	**0.12**

LME, respectively, and three of the eight parameters, characteristic velocity, wavelength, and elongation, are not significantly different between LMW and LME ($0.05 <$ p: probability value). The mean central latitude of the LME is 0.42 degrees higher than that of the LMW. The mean amplitude of the north-south meander of the LME is 0.10 degrees smaller than that of the LMW. The mean initial path direction of the LME is 8 degrees smaller than that of the LMW, which makes the amplitude smaller.

Figure 9 shows the latitudinal distribution of the direction (from the east) of the mean path east of Kyushu and south of Shikoku obtained by central difference ($\theta_i = \tan^{-1}\left(\frac{Y_{i+1} - Y_{i-1}}{2\Delta X}\right)$), as well as the initial path direction of the optimal solution at the central latitude. Both the mean path direction and the initial path direction decrease with latitude. In the central latitude range, 31.77° N to 32.41° N, except for 1975–1980, the decrease in initial path direction with increasing latitude is less than that in the mean path direction. The initial path direction depends on the central latitude, but differs slightly from the mean path direction, possibly due to the effect of the continental slope as well as elongation.

Whether the Kuroshio passes north or south of Hachijojima depends on the longitude of the trough, which divides the LMW and LME (see Fig. 7). The longitude of the trough is the sum of the longitude of the separation point, the elongation south of Shikoku and three-quarters of the wavelength. The mean longitude of the LME trough is 1.22 degrees larger than the mean longitude of the LMW trough (Table 2). Since there is no significant difference in wavelength and elongation between LME and LMW, the difference in longitude of the trough is generated by the 0.76 degrees' difference in longitude of the separation point. Although the wavelength depends on the characteristic velocity and the initial path direction, there is no sig-

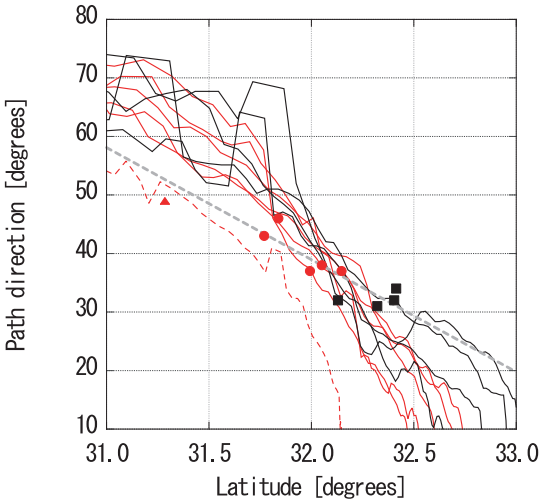

Fig. 9 Direction of the mean path at each latitude (lines) and the initial path direction of the optimal solution at the central latitude (marks). LMW (red) and LME (black). The dashed red line and triangle indicate 1975–1980 LMW. The gray dashed straight line represents the regression line for the nine marks except for the 1975–1980 LMW.

nificant difference in wavelength between LME and LMW because there is no significant difference in characteristic velocity and the dependence on the initial path direction is weak.

On the other hand, the longitude of the LMW trough for the 1975–1980 is 0.90 degrees less than the LMW mean. The large factors are the difference in elongation of 0.68 degrees and the difference in longitude of the separation point of 0.32 degrees. Elongation for the 1975–1980 period, when the path does not reach the 1000 m isobath south of Shikoku, is almost zero.

The 1981–1984 LME and LMW trough longitudes are nearly equal, almost in the middle of the LME mean and the LMW mean. This suggests that the trough of the 1981–1984 large meander alternated between LME and LMW paths because it was located near the boundary longitude where the LME and LMW are divided.

4. Discussion

The initial path direction and characteristic velocity were estimated by fitting solutions of the path equation to two types of Kuroshio large meanders, LMW and LME paths. A comparison of the five LMWs and three LMEs showed no significant differences in characteristic velocities and, therefore, no significant differences in meander wavelengths. The difference in the longitude of the meander troughs was due to the difference in the longitude at which the Kuroshio separates from the continental slope east of Kyushu or south of Shikoku. This differs from the estimation by White and McCreary (1976), who suggested that the troughs shift over the Izu-Ogasawara Ridge due to the increased velocity of the Kuroshio and the longer wavelengths of the Rossby lee waves.

As pointed out by Yoshida *et al.* (2014), at the last stage of the LMW-dominated large meander period, the Kuroshio path becomes the LME and transitions to the NLMS (non-large meander south), ending the large meander. This transition of the Kuroshio path can be seen as a northward shift of the separation latitude from the continental slope. The increase in Kuroshio volume transport at the last stage of the large meander period found by Tsujino *et al.* (2013) and Usui *et al.* (2013) may cause a northward shift in the separation latitude without an increase in characteristic velocities.

The path of the Kuroshio large meander deviates from the optimal solution of the path equation once it passes the trough, and flows northward over the western slope of the Izu-Ogasawara Ridge for LMW and over the eastern slope of the ridge for LME, mostly along the isobathic line. However, depths at the deviation points ranged from 4000 m and deeper in 1975–

1980 to approximately 1000 m near the top of the Izu-Ogasawara Ridge in some LMEs. This suggests that the deviation from the solution near the Izu-Ogasawara Ridge is not due to the local effect of the bottom topography.

Acknowledgments

We thank two reviewers for their helpful comments. For the Kuroshio path, we used the data digitized by the Japan Hydrographic Association of the QBOC issued by the Japan Coast Guard (JAPAN HYDROGRAPHIC ASSOCIATION, 2022). We used the bathymetric data ETOPO1 (AMANTE and EAKINS, 2009) provided by National Oceanic and Atmospheric Administration. We thank these institutions for their data. The Generic Mapping Tools version 6 (WESSEL *et al.*, 2019) was used to draw maps.

References

AMANTE, C. and B. W. EAKINS (2009): ETOPO1 1 arc-minute global relief model: procedures, data sources and analysis. NOAA Technical Memorandum NESDIS NGDC-24. Boulder, CO: National Geophysical Data Center.

AKITOMO, K., T. AWAJI and N. IMASATO (1991): Kuroshio path variation south of Japan: 1. Barotropic inflow-outflow model. Journal of Geophysical Research, **96** (C2), 2549–2560.

CHAO, S. -Y. (1984): Bimodality of the Kuroshio. Journal of Physical Oceanography, **14** (1), 92–103.

JAPAN HYDROGRAPHIC ASSOCIATION (2022): Kuroshio Current Path Dataset 2021 Ed. (1955–2021).

MASUDA, A. (1982): An interpretation of the bimodal character of the stable Kuroshio path. Deep Sea Research Part A. Oceanographic Research Papers, 29 (4), 471–484.

ROBINSON, A. R. and P. P. NIILER (1967): The theory of free inertial currents I. Path and structure. Tellus, **19** (2), 269–291.

ROBINSON, A. R. and B. A. TAFT (1972): A numerical experiment for the path of the Kuroshio. Journal of Marine Research, **30**, 65–101.

STOMMEL, H. and K. YOSHIDA (1972): Kuroshio; its physical aspects. Tokyo, University of Tokyo Press.

TSUJINO, H., S. NISHIKAWA, K. SAKAMOTO, N. USUI, H. NAKANO and G. YAMANAKA (2013): Effects of large-scale wind on the Kuroshio path south of Japan in a 60-year historical OGCM simulation. Climate Dynamics, **41**, 2287–2318.

TSUJINO, H., N. USUI and H. NAKANO (2006): Dynamics of Kuroshio path variations in a high-resolution GCM. Journal of Geophysical Research, **111** (C11), C11001.

USUI, N., H. TSUJINO, H. NAKANO and S. MATSUMOTO (2013): Long-term variability of the Kuroshio path south of Japan. Journal of Oceanography, **69**, 647–670.

WESSEL, P., J. F. LUIS, L. UIEDA, R. SCHARROO, F. WOBBE, W. H. F. SMITH and D. TIAN (2019): The Generic Mapping Tools version 6. Geochemistry, Geophysics, Geosystems, **20** (11), 5556–5564.

WHITE, W. B. and J. P. MCCREARY (1976): On the formation of the Kuroshio meander and its relationship to the large-scale ocean circulation. Deep Sea Research and Oceanographic Abstracts, **23** (1), 33–47.

YASUDA, I., J.-H. YOON and N. SUGINOHARA (1985): Dynamics of the Kuroshio large meander-barotropic model. Journal of the Oceanographical Society of Japan, **41**, 259–273.

YOON, J.-H. and I. YASUDA (1987): Dynamics of the Kuroshio large meander: two-layer model. Journal of Physical Oceanography, **17** (1), 66–81.

YOSHIDA, J., E. MAETA, N. NAKANO, H. DEGUCHI and M. NEMOTO (2014): Statistical analysis of the variation of the Kuroshio path, Oceanography in Japan, **23**, 171–196 (in Japanese with English abstract and legends)

Received: July 12, 2023
Accepted: October 26, 2023